Divergence of *germ cell-less* roles in germ line development across insect species

Authors: Jonchee A. Kao[1], Ben Ewen-Campen[2,3], Cassandra G. Extavour[1,2,4]

[1]Department of Molecular and Cellular Biology, Harvard University, 16 Divinity Ave, Cambridge, MA 02138, USA

[2]Department of Organismic and Evolutionary Biology, Harvard University, 16 Divinity Ave, Cambridge, MA 02138, USA

[3]Current address: Department of Genetics, Blavatnik Institute, Harvard Medical School, Harvard University, Boston, MA 02115, USA

[4]Howard Hughes Medical Institute, Chevy Chase, MD, USA

Corresponding author: Cassandra G. Extavour

Email: extavour@oeb.harvard.edu

Phone: (617) 496-1935

ORCIDs: JAK 0000-0003-1701-3265; BE-C 0000-0002-4326-3033, CGE 0000-0003-2922-5855

Keywords: *Oncopeltus fasciatus*; *Gryllus bimaculatus*; germ cell specification; *torso*; pole cells

Abstract

During development, sexually reproducing animals must specify and maintain the germ line, the lineage of cells that gives rise to the next generation of animals. In the fruit fly *Drosophila melanogaster*, *germ cell-less* (*gcl*) is required for the formation of primordial germ cells in the form of cells that cellularize at the posterior pole of the embryo, called pole cells. Forming pole cells is a mechanism of germ cell formation unique to a subset of insects. Even though most animals do not form pole cells as primordial germ cells, *gcl* is conserved across Metazoa, raising the question of how this conserved gene acquired its central role in the evolutionarily derived process of pole cell formation. Here, we examine the functions of *gcl* in two other insects with different modes of germ cell specification: the milkweed bug *Oncopeltus fasciatus* and the cricket *Gryllus bimaculatus*. We found that *gcl* is involved in germ cell development, but not strictly required for germ cell specification, in *O. fasciatus*, although it appears to function through a mechanism different from that in *D. melanogaster*. In contrast, we could not detect any impact on the embryonic germ line upon *gcl* knockdown in *G. bimaculatus*. This work serves as a case study into how the roles of genes in the process of germ line development can change over evolutionary time across animals.

Keywords: Germ cells; pole cells; *Oncopeltus fasciatus*; *Gryllus bimaculatus*; Hemimetabola; milkweed bug; cricket; Torso

Highlights

- *germ cell-less* knockout reduces germ cell number in *Oncopeltus fasciatus*.
- *germ cell-less* knockdown does not affect germ cell number in *Gryllus bimaculatus*.
- The genetic mechanisms through which *gcl* affects germ cell number have diverged among insects.

Graphical abstract

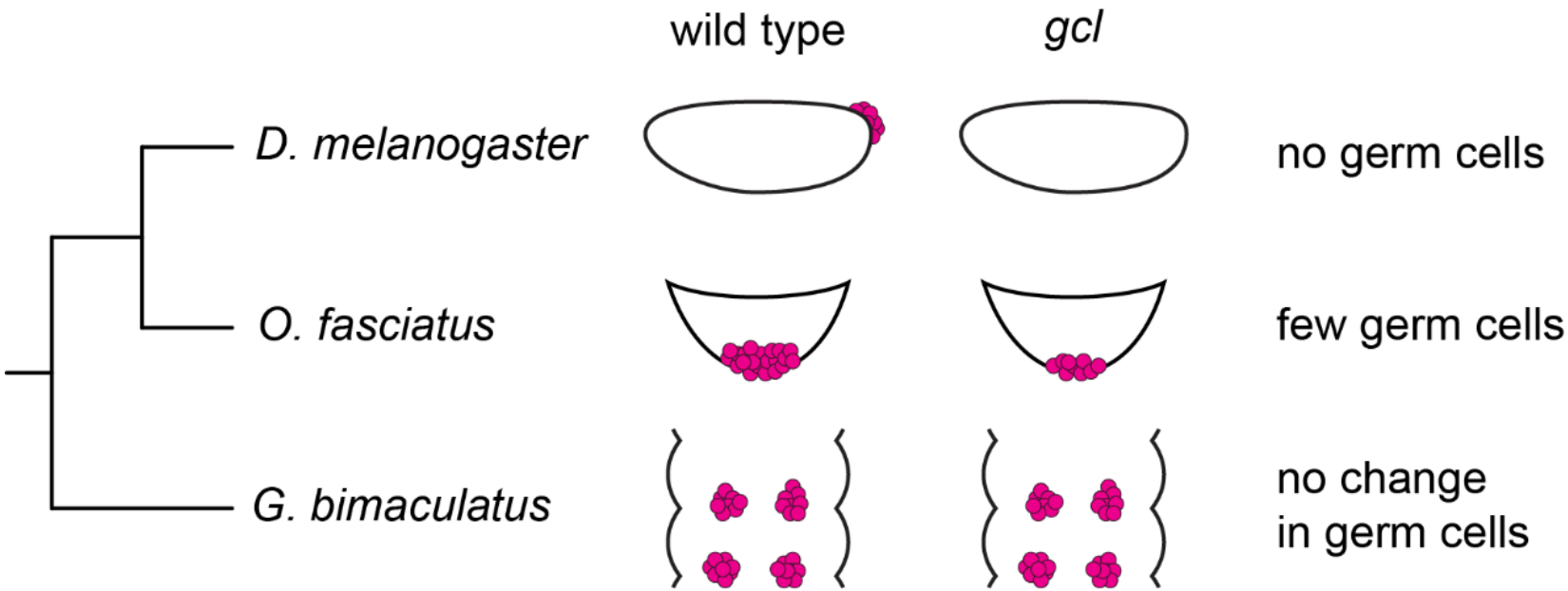

48 **Introduction**

49 One of the most crucial processes in animal development is the specification and
50 maintenance of the germ line, the lineage of cells uniquely capable of giving rise to the next
51 generation of animals (Extavour and Akam, 2003). Despite the importance of this process,
52 mechanisms of germ line development vary widely even within closely related taxa, including
53 across insects (Extavour and Akam, 2003). For example, in the fruit fly *Drosophila*
54 *melanogaster*, germ cells first appear at the posterior pole of the embryo very early in
55 embryogenesis, before cellularization occurs in the rest of the embryo (Huettner, 1923). The
56 formation of germ cells in embryos of this fly depends on the presence of the germ plasm, a
57 specialized region of the cytoplasm at the posterior pole containing maternally synthesized
58 RNAs and proteins that collectively direct the formation and specification of germ cells
59 (Illmensee and Mahowald, 1974). In contrast, germ cells in the cricket *Gryllus bimaculatus* are
60 first detectable comparatively later in embryogenesis, after segmentation of the abdomen has
61 begun (Ewen-Campen et al., 2013a). There is no evidence of germ plasm in cricket embryos, and
62 germ cells are thought to be specified instead by inductive signals from neighboring cells,
63 including BMP signaling (Donoughe et al., 2014; Ewen-Campen et al., 2013a). In yet another
64 mechanism of insect germ cell specification, germ cells of the milkweed bug *Oncopeltus*
65 *fasciatus* appear at a stage intermediate between those of *D. melanogaster* and *G. bimaculatus*,
66 after blastoderm cellularization but before abdominal segmentation (Butt, 1949; Ewen-Campen
67 et al., 2013b). There is also no evidence of germ plasm in embryos of this bug (Ewen-Campen et
68 al., 2013b), but specific germ cell specification signals have not been identified.

69 Despite the variation in modes of germ line development across species, many genes
70 involved in this process are conserved. These include *vasa* and *piwi*, which are commonly used

71 as germ cell markers in many different animals (Ewen-Campen et al., 2010). *germ cell-less* (*gcl*)
72 is also sometimes used as a germ cell marker, but its role in germ line development is less well
73 understood (Jongens et al., 1992). Embryos laid by *D. melanogaster* females homozygous for a
74 loss of function mutation in *gcl* have significantly fewer germ cells than controls, if any (Jongens
75 et al., 1994, 1992). The gene is thought to have a role in suppressing somatic cell fate by
76 targeting the receptor tyrosine kinase Torso for degradation (Colonnetta et al., 2021; Pae et al.,
77 2017). *gcl* is also required for germ cell transcriptional quiescence in flies (Leatherman et al.,
78 2002). However, *gcl* is not required for germ cell specification in the mouse *Mus musculus* nor in
79 the flour beetle *Tribolium castaneum*, but it is required for proper mouse spermatogenesis
80 (Ansari et al., 2018; Kimura et al., 2003). Outside the germ line, *gcl* plays a role in establishing
81 the anterior–posterior axis in *T. castaneum* (Ansari et al., 2018). Despite the wide divergence in
82 their physiological roles, *gcl* homologs are highly conserved in amino acid sequence, with 45%
83 similarity between homologs from *D. melanogaster* and *M. musculus*. In addition, these
84 homologs appear to share at least some biochemical functions, since the mouse *gcl* homolog can
85 partially restore germ cell formation in a *gcl*-null *D. melanogaster* embryo, though not to wild
86 type numbers (Leatherman et al., 2000). *gcl* expression has also been observed in the embryonic
87 germ line in other arthropod species (Ewen-Campen et al., 2013a; Gupta and Extavour, 2013).
88 However, to our knowledge, functional tests of whether *gcl* is required for insect germ line
89 development or function remain limited to *D. melanogaster* and *T. castaneum*.

90 Here, we examine the function of *germ cell-less* in the embryonic and adult germ lines of
91 *O. fasciatus* and *G. bimaculatus*. Our data suggest that *gcl* is not required for germ cell
92 specification nor for adult gametogenesis in either species. However, *gcl* mutant *O. fasciatus*
93 embryos have significantly fewer germ cells than wild type. Knockdown of *Of-torso* does not

affect germ cell number, suggesting that *gcl* in this species affects germ cell number through a different mechanism from that in *D. melanogaster*. Overall, these studies into *gcl* function across species inform our understanding of the evolution of gene function in germ line development.

Materials and Methods

Gene identification

germ cell-less. *Of-germ cell-less* is annotated as OFAS015300 on Scaffold 2113 of the current *O. fasciatus* genome assembly (Panfilio et al., 2019). *Gb-germ cell-less* is annotated as GBIM03474 on Scaffold 14 of the current *G. bimaculatus* genome assembly (Ylla et al., 2021). We amplified both genes from mixed stage embryonic cDNA of the respective species to verify the full-length coding sequences.

Of-torso. A tBLASTn search was performed on the *O. fasciatus* genome (Panfilio et al., 2019) using *D. melanogaster* Torso as a query, and a reciprocal BLASTp was performed on the top results with e-value < 1e–40. Of the initial results, OFAS005359 on Scaffold 336 returned *torso* orthologs from other insects. A reciprocal BLASTp search using the adjacent upstream annotated gene, OFAS005360, also returned *torso* orthologs from other insects. PCR was performed from mixed stage embryonic cDNA to confirm that OFAS005359 and OFAS005360 correspond to the same transcript. To obtain full-length sequence, RACE was performed using the SMARTer RACE 5’/3’ Kit (Takara Bio 634859) following manufacturer’s instructions.

The initial tBLASTn search using *D. melanogaster* Torso as a query also returned OFAS025175 as a result. A reciprocal BLASTp search using the predicted peptide sequence of this hit returned *fgf receptor* orthologs from other insects. Since the FGF receptor is a family of

116 receptor tyrosine kinases closely related to Torso (Duncan et al., 2013), we wanted to include
117 OFAS025175 for phylogenetic analysis. Therefore, we performed RACE using the SMARTer
118 RACE 5'/3' Kit to obtain the full-length sequence of this gene. Full length sequences for both
119 *Of-torso* and *Of-fgfr* have been deposited at GenBank with accession numbers PV361543 and
120 PV361544, respectively.

121 Phylogenetic analysis was performed using MEGA 11 (Tamura et al., 2021). Insect
122 orthologs of Torso were aligned using MUSCLE (Edgar, 2004) along with orthologs of Ret
123 oncogene and FGF receptor, which are the closest related families of receptor tyrosine kinases
124 (Duncan et al., 2013). The multiple sequence alignment was used to generate a gene tree using
125 the Maximum Likelihood method with the JTT substitution model (Jones et al., 1992), a discrete
126 Gamma-distributed rate model and 1000 bootstrap replicates.

127

128 *Molecular biology*

129 *RNA extraction and cDNA synthesis*. Embryos or tissues of interest were homogenized in TRIzol
130 (Invitrogen 15596026), and RNA was extracted with phenol–chloroform extraction and
131 isopropanol precipitation. cDNA was synthesized with SuperScript III First-Strand Synthesis
132 SuperMix for qRT-PCR (Invitrogen 11752250) following manufacturer's instructions.

133 *Cloning and* in vitro *transcription.* Fragments of genes of interest were PCR-amplified from
134 embryonic cDNA and each cloned into the pGEM-T Easy vector (Promega A137A) using
135 manufacturer's instructions. A fragment of *gfp* was subcloned from an existing plasmid
136 containing the *gfp* sequence. Insertion was confirmed by Sanger sequencing. Primers used are
137 listed in Supplemental Table 1.

138 For *in situ* probe synthesis, gene fragments were PCR-amplified from plasmids using T7
139 and Sp6 primers. *In vitro* transcription was performed using T7 RNA polymerase (Promega
140 P2075) or Sp6 RNA polymerase (Roche 10810274001) with DIG RNA labeling mix (Roche
141 11277073910). 100 ng of template was used for a 20-µl reaction run at 37°C overnight. RNA
142 was purified with LiCl/ethanol precipitation, then resuspended in 20 µl DEPC-treated water.
143 Concentration was measured using a NanoDrop Spectrophotometer (ThermoFisher), and the
144 sample was diluted to 100 ng/µl with hybridization buffer (50% formamide, 1x phosphate-
145 buffered saline (PBS), 5x saline–sodium citrate (SSC), 0.1% Triton X-100, 0.1% CHAPS, 5 mM
146 EDTA, 50 µg/mL heparin, 1 µg/mL yeast tRNA). Probes were stored at −20°C.

147 For double-stranded RNA (dsRNA) synthesis, gene fragments were PCR-amplified from
148 plasmids using a forward T7 primer and a reverse primer containing both T7 and Sp6 promoter
149 sequences to generate a template for *in vitro* transcription with the T7 promoter sequence on both
150 ends. *In vitro* transcription was performed using the MEGAscript T7 Transcription Kit
151 (Invitrogen AM13345). 100 ng of template was used for an 80-µl reaction run at 37°C overnight.
152 RNA was purified with LiCl/ethanol precipitation, then resuspended in 100 µl DEPC-treated
153 water. To anneal the two strands, this solution was heated to 95°C on a heat block for 5 minutes,
154 then allowed to cool slowly by leaving the tube on the heat block with the power switched off. A
155 1:10 dilution of annealed RNA was analyzed using a NanoDrop Spectrophotometer
156 (ThermoFisher) to measure its concentration and purity, then run on a 1% agarose gel to confirm
157 its size and integrity. For embryonic RNAi, dsRNA was diluted in DEPC-treated water to 2 µg/µl
158 (*O. fasciatus*) or 5 µg/µl (*G. bimaculatus*), with 0.05% phenol red. For *G. bimaculatus* adult
159 RNAi, dsRNA was diluted to 7.5 µg/µl in DEPC-treated water.

160 *CRISPR/Cas9-mediated mutagenesis*. Alt-R S.p. Cas9 Nuclease V3 (cat. #1081059) and Alt-R
161 CRISPR-Cas9 tracrRNA (cat. #1072533) were ordered from IDT, along with gene-specific Alt-R
162 CRISPR-Cas9 crRNA. tracrRNA and crRNA were resuspended to 100 µM in Nuclease-Free
163 Duplex Buffer (IDT cat. #11-01-03-01). 5 µl of each RNA were combined in a PCR tube, heated
164 to 95°C for 5 minutes, and allowed to cool to room temperature to form 50 µM gRNA duplex. 3
165 µl gRNA and 2 µl Cas9 protein (10 µg/µl or ~62 µM) were combined in a PCR tube and
166 incubated at room temperature for 10 minutes to form Cas9/gRNA ribonucleoprotein complex
167 (RNP) at roughly 25 µM. Finally, RNP was diluted tenfold in 1x PBS with 0.05% phenol red.

168

169 *Of-Vasa antibody generation*

170 A rabbit polyclonal antibody was raised against a recombinant *Of*-Vasa protein fragment
171 (McGill Biology CIAN facility, Canada). The sequence encoding the 565 C-terminal amino acids
172 of *Of*-Vasa, the stop codon and the first 96 base pairs of 3' UTR (GenBank accession KC261571
173 (Ewen-Campen et al., 2013b)) was cloned into the pET151/dTOPO expression vector (Invitrogen
174 K151-01), thus introducing an N-terminal 6x-polyhistidine tag. Protein expression was induced
175 in *E. coli* BL21 (DE3) by addition of IPTG to a final concentration of 0.25 mM and shaking at
176 30°C for four hours. The overexpressed proteins were highly insoluble, so the cell pellets were
177 disrupted by sonication in non-denaturing buffer, and the soluble fraction was separated by
178 centrifugation and discarded. The pellet was resuspended in 8 M urea (crude prep). Crude preps
179 were further purified by SDS gel-purification. Protein bands were excised from the gel after
180 reverse staining with zinc chloride and the proteins were collected by electroelution. Acetone
181 precipitation was performed, and the precipitated protein was washed and resuspended in 8 M
182 urea. Protein concentration was adjusted to 1–2 mg/mL for injection. Rabbits were injected using

183 a standard 80-day protocol with three boosts after the initial injection; the final bleed was
184 performed after 87 days. The serum was processed by addition of sodium azide to 0.02% (w/v).
185 The antibody was affinity-purified against bacterially expressed *Of*-Vasa protein.

186

187 *Embryo microinjection*

188 Needles for injection were made by pulling glass capillaries (World Precision Instruments
189 1B100-4) with a Sutter P-97 Flaming/Brown micropipette puller. Needle tips were manually
190 opened with fine forceps just prior to injection. Eggs were injected with a Narishige IM300
191 microinjector.

192 *O. fasciatus* were allowed to lay eggs in dry cotton for four hours, after which eggs were
193 picked out of the cotton for injection. Two glass microscope slides were taped together with
194 double-sided tape to create a ledge with exposed double-sided tape against which embryos were
195 lined up. Eggs were then submerged in tap water for at least 20 minutes to soften the eggshell
196 before injection. Slides with injected eggs were kept at 28°C to continue development until the
197 desired age.

198 *G. bimaculatus* were allowed to lay eggs in wet cotton for four hours, after which eggs
199 were washed out of the cotton for injection. Eggs were aligned in grooves (570 µm wide × 2930
200 µm long × 650 µm deep) made in 2% agarose in Milli-Q water using a custom mold as
201 previously described (Donoughe et al., 2018). Eggs were injected while submerged in 1x PBS.
202 After injection, the solution was replaced with fresh 1x PBS. Injected eggs were kept submerged
203 in 1x PBS at 28°C overnight. The following day, dead embryos, if any, were removed, and the
204 remaining eggs were transferred onto damp Kimwipes in a covered Petri dish kept at 28°C to

205 continue development. Three days after injection, eggs were submerged in tap water again and
206 monitored every day until they reached the desired stage for dissection.

207

208 *Embryo dissection and fixation*

209 *O. fasciatus* eggs were stuck to the bottom of a 60-mm Petri dish with double-sided tape
210 and a slit was created in the eggshell with a microscalpel. 1x PBS with 4% paraformaldehyde
211 (PFA) was then poured into the dish to fix the embryos for 30 minutes at room temperature,
212 followed by at least three washes with PBT (1x PBS with 0.1% Triton X-100). Embryos were
213 then dissected free of their yolk in PBT with fine forceps. Embryos were washed at least three
214 times with PBT at room temperature before continuing with staining or dehydration in methanol.

215 *G. bimaculatus* embryos were dissected free of their yolk in 1x PBS with fine forceps and
216 fixed overnight in 1x PBS with 4% PFA at 4°C. The following morning, they were washed at
217 least three times with PBT at room temperature before continuing with staining or dehydration in
218 methanol.

219

220 *G. bimaculatus adult RNA interference (RNAi)*

221 2 µl dsRNA was injected into the abdomen of an adult cricket with a Hamilton syringe
222 through the base of a metathoracic leg. Gonads were dissected seven days after injection for
223 analysis.

224

225 *Colorimetric in situ hybridization*

226 Dissected embryos were stored in methanol at −20°C overnight or longer before *in situ*
227 hybridization. After rehydration in PBT and washing in hybridization buffer, embryos were
228 hybridized overnight in a 70°C water bath with 1 ng/µl probe in hybridization buffer. The
229 following day, the following series of 20-minute washes were performed at 70°C: once in
230 hybridization buffer, three times in wash 1 (2x SSC, 0.1% CHAPS) and three times in wash 2
231 (0.2x SSC, 0.1% CHAPS). Embryos were then washed three times for ten minutes each at room
232 temperature in KTBT (1x Tris-buffered saline with KCl and 0.1% Triton X-100) followed by an
233 hour-long incubation at room temperature in *in situ* blocking solution (1x PBS, 0.1% Tween-20,
234 5% NGS, 2 mg/mL bovine serum albumin, 1% dimethyl sulfoxide). Embryos were incubated for
235 two hours at room temperature with sheep anti-digoxigenin–AP (Roche 11093274910), diluted
236 1:2000 in *in situ* blocking solution, then washed at least four times over two hours with KTBT
237 and incubated in KTBT overnight at 4°C. The following day, embryos were washed with NTMT
238 (100 mM Tris pH 9.5, 100 mM NaCl, 50 mM $MgCl_2$, 0.1% Tween-20), then developed in the
239 dark at 37°C with NBT/BCIP in NTMT with 5% polyvinyl alcohol. Development was monitored
240 at least every hour under a dissection microscope. To stop development of the enzymatic
241 reaction, embryos were washed in PBT, incubated with 5 ng/µl Hoechst 33342 in PBT at room
242 temperature for an hour, post-fixed in 4% PFA in PBS, then incubated in 70% glycerol before
243 mounting in 100% glycerol.

244

245 *Immunohistochemistry*

246 Embryos were incubated in blocking solution (PBT with 5% normal goat serum (Jackson
247 ImmunoResearch 005-000-121)) for one hour at room temperature, then incubated overnight at

248 4°C with primary antibodies diluted in blocking solution. The following day, embryos were
249 washed for at least four times over four hours with PBT, incubated for an hour in blocking
250 solution, then incubated overnight at 4°C with secondary antibodies diluted in blocking solution.
251 Finally, embryos were washed in PBT, post-fixed in 4% PFA in PBS, then incubated in 70%
252 glycerol before mounting in glycerol. Antibody staining was also performed with a no-primary
253 control.

254 Primary antibodies used were: rabbit anti-*Gb*-Piwi (Ewen-Campen et al., 2013a) at a final
255 concentration of 1:300; rabbit anti-*Of*-Vasa at 1:100; mouse anti-α-tubulin (DM1A; Sigma
256 T9026) at 1:100; rabbit anti-β-catenin (Sigma C2206) at 1:500; and mouse anti-RNA polymerase
257 II (H5; Covance MMS-129R) (Bregman et al., 1995; Warren et al., 1992) at 1:100. Secondary
258 antibodies used were goat anti-rabbit conjugated to Alexa Fluor 647 (Invitrogen A-21246), goat
259 anti-rabbit Alexa Fluor 488 (Invitrogen A-11008), goat anti-rabbit Alexa Fluor 568 (Invitrogen
260 A-11011), donkey anti-mouse Alexa Fluor 488 (Invitrogen A-21202), and goat anti-mouse Alexa
261 Fluor 647 (Invitrogen A-21236). All secondary antibodies were used at a final concentration of
262 1:400 along with Hoechst 33342 (Sigma B2261) at 5 ng/µl.

263 Embryos were imaged on a Nikon CSU-W1 spinning disk inverted confocal microscope
264 with 10x air or 20x air objectives or a Zeiss AxioObserver inverted compound microscope with
265 10x air or 20x air objectives. Images were analyzed in Fiji.

266

267 *Quantitative RT-PCR*

268 Quantitative RT-PCR was performed on an AriaMx Real-time PCR system (Agilent)
269 using PerfeCTa SYBR Green SuperMix, Low ROX (Quantabio 95056). Fold-change differences

270 were calculated using the $\Delta\Delta C_t$ method for RNAi experiments. Expression levels were
271 normalized against *Of-gapdh* or *Gb-β-tubulin*. All primers used are listed in Supplemental Table
272 1.

273 **Results**.

274 *germ cell-less expression across insect species.*

275 During oogenesis in *D. melanogaster*, Gcl protein is detectable at the nuclear membrane
276 of nurse cells and oocytes (Moore et al., 2009). In addition, *gcl* transcripts are transcribed by
277 nurse cells, transported into the oocyte and deposited at the oocyte posterior, where they remain
278 as part of the germ plasm into early embryogenesis (Jongens et al., 1992). These transcripts are
279 translated into protein starting at the cleavage stages of embryogenesis (Jongens et al., 1992).
280 Gcl protein is localized to the nuclear membranes of germ cells after they form and remains
281 detectable in germ cells until mid-gastrulation, when germ cells enter the primordial midgut
282 (Jongens et al., 1992). We asked whether *gcl* is also expressed in other insect embryos at the time
283 and place of germ cell specification.

284 We (Ewen-Campen 2013) and others (Butt 1949) have qualitatively described the first
285 appearance of primordial germ cells in blastoderm stage *O. fasciatus* embryos, and their
286 proliferation and migration during embryogenesis. However, to our knowledge there has been no
287 embryonic developmental staging system established for this insect. We therefore we defined
288 stages based on major embryological, morphogenetic and morphological milestones, for
289 describing embryonic development from egg-laying through to katatrepsis, with special
290 emphasis on the development of germ cells (Supplemental Figure 1; Supplemental Table 2). We
291 assessed *gcl* transcript levels using quantitative RT-PCR on *O. fasciatus* embryos collected in 12-

292 hour windows spanning the first four days of embryogenesis. *Of-gcl* transcripts were detected at
293 the highest levels 24–36 hours after egg-lay at 28°C (Figure 1A). This window corresponds to
294 the late blastoderm stage (stage 3), when germ cells are first distinguishable (Ewen-Campen et
295 al., 2013b), and the beginning of germ band elongation (stages 4–5). We speculate that this peak
296 in expression is likely due to zygotic rather than maternal expression, since it is higher than
297 expression in freshly laid eggs. However, we were unable to detect *Of-gcl* transcripts by *in situ*
298 hybridization above background levels in embryos at any stage of development, nor in adult
299 ovaries or testes (Supplemental Figure 2A–B).

300 We similarly assessed *gcl* transcript levels using qRT-PCR on *G. bimaculatus* embryos
301 collected in 8-hour windows spanning the first two days of embryogenesis and 24-hour windows
302 spanning the following eight days of embryogenesis. *Gb-gcl* transcripts were detectable at the
303 highest levels in the first eight hours after egg-lay (Figure 1B), suggesting maternal deposition of
304 *Gb-gcl* transcript. Consistent with this hypothesis, *Gb-gcl* transcript was detectable by *in situ*
305 hybridization in ovaries but not during embryogenesis (Supplemental Figure 2C–D).

306 Although we were unable to detect localized *gcl* expression in either *O. fasciatus* or *G.*
307 *bimaculatus* embryos, we still sought to determine whether the gene's documented roles in germ
308 cell specification (*D. melanogaster*) or adult spermatogenesis (*M. musculus*) might be conserved
309 (Jongens et al., 1992; Kimura et al., 2003). To this end, we analyzed *gcl* loss of function
310 conditions in embryos and adult gonads of both species. *gcl* is also required for transcriptional
311 quiescence in germ cells in *D. melanogaster* (Leatherman et al., 2002). However, we could not
312 detect any reduction in transcriptional activity in germ cells relative to somatic cells of either *O.*
313 *fasciatus* or *G. bimaculatus* (Supplemental Figure 3), so we did not assess this phenotype in our
314 functional studies of *gcl*.

315

316 *Of-gcl mutation decreases germ cell number in milkweed bug embryos.*

317 To determine whether *gcl* is required for germ cell specification in *O. fasciatus*, we
318 generated an *Of-gcl* putative protein-null allele with CRISPR/Cas9-mediated mutagenesis
319 (Figure 2A–B). This allele contains a 2-bp insertion at amino acid residue 14. The resulting
320 frameshift leads to a premature stop codon, resulting in a predicted peptide of 30 amino acid
321 residues, compared with the 478-residue wild type protein. Surprisingly, individuals homozygous
322 for this mutant allele were viable and fertile, and we have maintained a stable mutant line for at
323 least twelve generations at the time of writing. There were no detectable morphological defects
324 in adult ovaries or testes from this mutant line, nor any evidence of abnormal gametogenesis in
325 either males or females (Supplemental Figures 4–5).

326 In *O. fasciatus*, germ cells are first detectable in stage 3 on the interior of the cellular
327 blastoderm, forming part of an invaginating structure called the posterior pit (Ewen-Campen et
328 al., 2013b). The germ cells remain at the posterior end of the germ band as it forms by
329 invaginating into the egg (Ewen-Campen et al., 2013b) (Figure 2B; Supplemental Figure 1). At
330 stage 3, *gcl* mutant embryos had on average 35% fewer germ cells than wild type embryos ($p <$
331 0.001; $n = 14$ wild type, 8 *gcl* embryos; Figure 2C–D; Supplemental Table 3). Germ cell number
332 remained significantly lower in *gcl* mutant embryos relative to wild type embryos throughout all
333 embryonic stages examined (Figure 2D). We detected a marginal decrease in germ cell
334 proliferation in *gcl* mutant embryos relative to wild type only at stages 6 and 9, as measured by
335 the proportion of germ cells with detectable phospho-histone 3 (Figure 2E; Supplemental Table
336 3). However, there was no detectable difference in germ cell proliferation between the two
337 genotypes at any other embryonic stage examined (Figure 2E; Supplemental Table 3). We were

338 also unable to detect cleaved caspase 3-dependent cell death in stages 3–4 of either genotype (*n* =
339 27 wild type, 23 *gcl* embryos).

340 It is formally possible that *gcl* loss of function affects the expression of Vasa protein,
341 which we use as an experimental proxy for identifying germ cells. However, we noted that the
342 Vasa-positive cells in *gcl* mutant embryos expressed Vasa at comparable levels to wild type
343 embryos. Thus, while we cannot rule out the possibility that germ cells that do not express
344 detectable Vasa may be present in our *gcl* loss of function embryos, we believe it unlikely that
345 lack of *gcl* would eliminate Vasa expression in some germ cells without significantly affecting
346 expression in others. Therefore, we favor the interpretation that the reduction in Vasa-positive
347 cells in *gcl* mutant embryos reflects a reduction in germ cell number. Given that the discrepancy
348 in germ cell number did not appear to be the result of differences in cell proliferation or cell
349 death, these data suggest that *Of-gcl* is involved in, but not strictly necessary for, one or more of
350 germ cell specification, formation or maintenance.

351 In *D. melanogaster*, Gcl promotes germ cell fate by targeting the receptor Torso for
352 degradation, and *torso* RNAi in *gcl* mutant flies restores germ cell numbers to wild type levels
353 (Pae et al., 2017). To determine whether this mechanism of germ cell number determination is
354 conserved in *O. fasciatus*, we asked whether *torso* loss of function also affects germ cell number
355 in this species. Despite previous reports that the *O. fasciatus* genome lacks a *torso* ortholog
356 (Skelly et al., 2019; Weisbrod et al., 2013), we identified a high-confidence homolog in the
357 published genome assembly (Panfilio et al., 2019) (Figure 3A). Knockdown of *Of-torso* by
358 embryonic RNAi did not affect germ cell number in stages 3–4 in either wild type or *gcl* mutant
359 backgrounds (Figure 3B–C). qPCR analysis of injected embryos confirmed that RNAi was
360 effective at reducing *torso* transcript levels to 50% relative to controls (Supplemental Figure 6A).

361 This result suggests that the mechanism through which *gcl* controls germ cell number is not
362 conserved between *O. fasciatus* and *D. melanogaster*.

363

364 *Gb-gcl knockdown does not affect germ cell number in cricket embryos.*

365 To determine whether *gcl* is required for germ cell specification in *G. bimaculatus*, we
366 knocked down *gcl* expression using embryonic RNAi. We found no significant difference in total
367 germ cell number in stage 8 embryos under *gcl* knockdown relative to *gfp* controls, nor did we
368 detect any significant difference in germ cell number in any segment (Figure 4). qPCR analysis
369 of injected embryos confirmed that RNAi was effective at reducing *gcl* transcript levels to 34%
370 relative to controls (Supplemental Figure 6B). It is possible that knockdown efficiency is not
371 high enough with RNAi to affect germ cell specification. However, we note that we have
372 previously detected significant changes in germ cell number with comparable or lower
373 knockdown efficiencies (Barnett et al., 2019; Donoughe et al., 2014; Nakamura and Extavour,
374 2016). Therefore, we speculate that the role of *Gb-gcl* in germ cell specification or maintenance,
375 if any, must be subtle.

376 Next, we asked whether *gcl* has any role in adult gametogenesis in *G. bimaculatus* by
377 performing RNAi in adult crickets. We could not detect any morphological or gametogenesis
378 defects in either ovaries or testes (Supplemental Figures 4-5). These data suggest that *gcl* is not
379 required for adult gametogenesis in this cricket.

380

381 **Discussion**.

382 Our analysis of *gcl* loss of function in embryos of two different hemimetabolous insects
383 suggests that *gcl* is not required for germ cell specification in these species, in contrast to the
384 gene's importance in germ cell formation in *D. melanogaster*. However, *Of-gcl* knockout
385 embryos have significantly fewer germ cells than wild type embryos, suggesting that the gene
386 may be involved in germ cell specification or maintenance in this bug, even if it is not strictly
387 required.

388 Gcl protein suppresses the somatic cell fate in *D. melanogaster* by targeting the receptor
389 tyrosine kinase Torso for degradation (Colonnetta et al., 2021; Pae et al., 2017). Germ cell
390 number can thus be modulated in flies by up- or downregulating Torso activity (Pae et al., 2017).
391 However, RNAi knockdown of *torso* in *O. fasciatus* does not affect germ cell number in either
392 wild type or *gcl* mutant embryos (Figure 3). Therefore, we hypothesize that germ cell
393 specification in this species does not require downregulation of Torso by Gcl, and that *Of-gcl*
394 regulates germ cell specification through some other unknown pathway. Torso's role in germ cell
395 specification may have been co-opted from its ancestral functions in neuroendocrine signaling,
396 just as it is thought to have been co-opted into its role in terminal patterning in flies (Duncan et
397 al., 2013; Schoppmeier and Schröder, 2005).

398 In *D. melanogaster*, the interaction between Gcl and Torso proteins depends on sequence
399 motifs present on both proteins (Pae et al., 2017). In Gcl protein, this motif is the GCL domain,
400 which is conserved across insect homologs (Supplemental Figure 7) (Pae et al., 2017). Torso
401 interacts with Gcl through a motif in the linker domain between its split kinase domains. This
402 linker region is significantly longer in *Dm*-Torso compared with other insect homologs
403 (Supplemental Figure 8), and the specific motif identified by Pae and colleagues (Pae et al.,

404 2017) is not present in other homologs. The conservation of the GCL domain despite the lack of
405 conservation in the Torso interaction motif may suggest that Gcl has some other unknown
406 interaction partner, or that the Gcl–Torso interaction may not be as sequence-specific as
407 originally thought. AlphaFold3 (Abramson et al., 2024) predicts potential interaction between
408 Gcl and Torso homologs in both *O. fasciatus* and *G. bimaculatus* through the split kinase linker
409 domain of Torso (Supplemental Figure 9). Further experiments will be needed to test whether
410 these proteins interact *in vivo*, and to identify additional conserved interaction partners of Gcl.

411 In mice, *gcl* knockout results in abnormal nuclear morphology in the liver, pancreas and
412 testis, though the only functional defect identified was impaired spermatogenesis (Kimura et al.,
413 2003). Similarly, *gcl* is expressed at low levels in somatic tissues in flies including the gut,
414 muscle and nervous system, but no defects have been reported in those tissues in *gcl*-null flies
415 (Jongens et al., 1992; Robertson et al., 1999). We were also unable to detect any defects in
416 spermatogenesis under either *Of-gcl* knockout or *Gb-gcl* knockdown conditions (Supplemental
417 Figure 4). Given that the mouse *gcl* homolog can rescue germ cell formation in *gcl*-null flies
418 (Leatherman et al., 2000), its biochemical functions are likely to be conserved across these
419 species. We speculate that *gcl* has a ubiquitous but subtle cell biological role in maintaining
420 nuclear morphology that only yields a phenotype in certain tissue contexts, such as in mouse
421 spermatogenesis. Under this hypothesis, *gcl* then gained an additional role in germ cell
422 specification in certain lineages of insects. In addition, the mechanism underlying this germ cell
423 specification has diverged between insect lineages, perhaps through the evolution of new
424 interaction partners such as Torso. This model reflects the complexity and variation present in the
425 mechanisms of germ cell specification and their evolution, including the co-option of new genes
426 with the shifting mechanisms of this process across animals.

Author contributions

JAK: Conceptualization, Methodology, Formal Analysis, Investigation, Writing – Original Draft, Writing – Review & Editing, Visualization; BE-C: Resources; CGE: Conceptualization, Writing – Review & Editing, Supervision, Funding Acquisition

Acknowledgments

The authors thank members of the Extavour lab for valuable discussions. This research was supported by National Science Foundation (NSF) Awards IOS-2220747 and IOS-0817678 to CGE, and an NSF Graduate Research Fellowship to BE-C. CGE is a Howard Hughes Medical Institute Investigator.

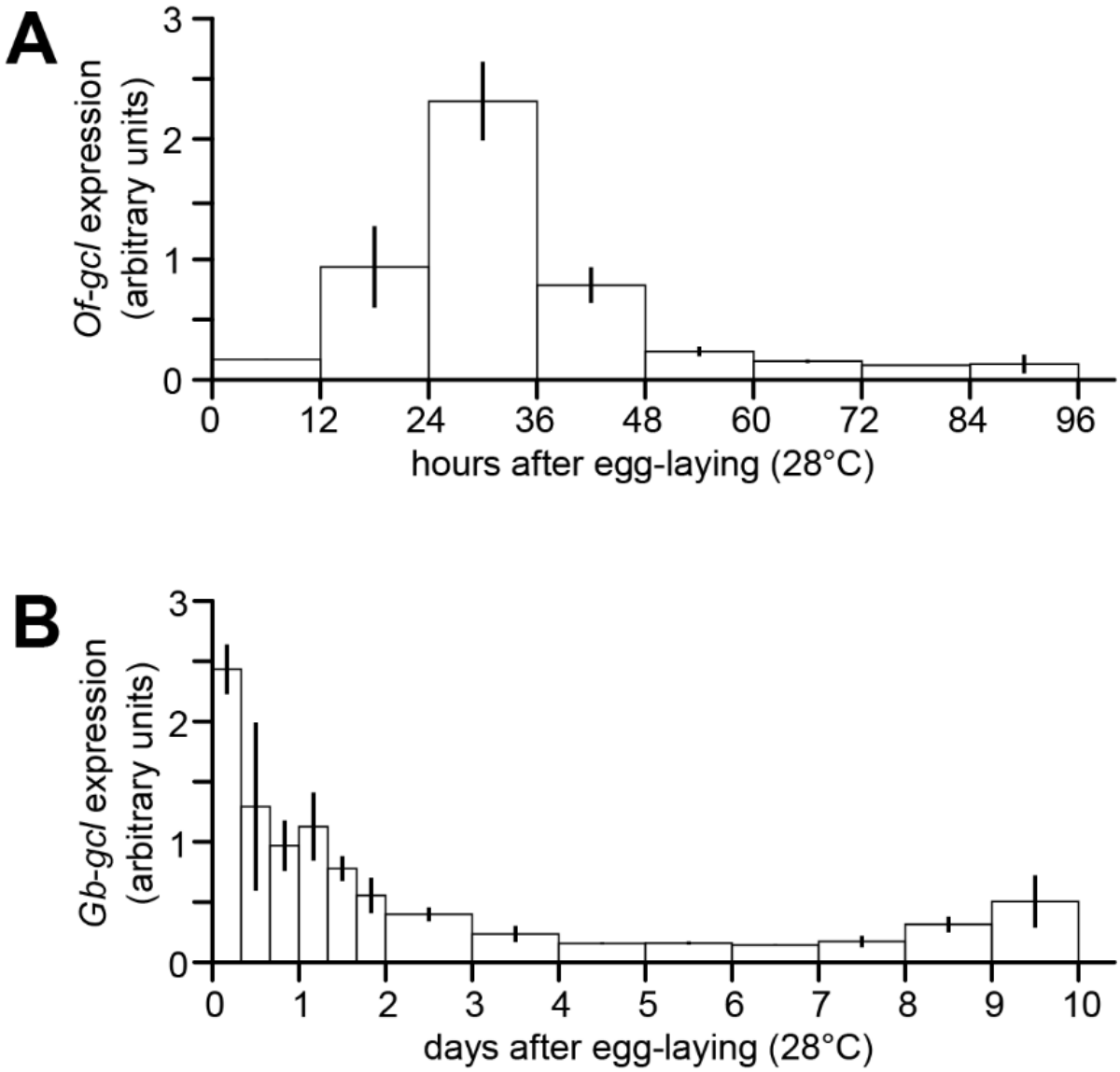

438

439 **Figure 1. *gcl* expression is detectable by qPCR in *O. fasciatus* (A) and *G. bimaculatus* (B)**
440 **embryos.** C_q values were normalized against *Of-gapdh* or *Gb-tubulin* expression and averaged
441 over four biological replicates for each time point. Error bars represent standard deviations. The
442 width of each bar represents the length of time for each embryo collection.

443

444 **(single column width)**

445

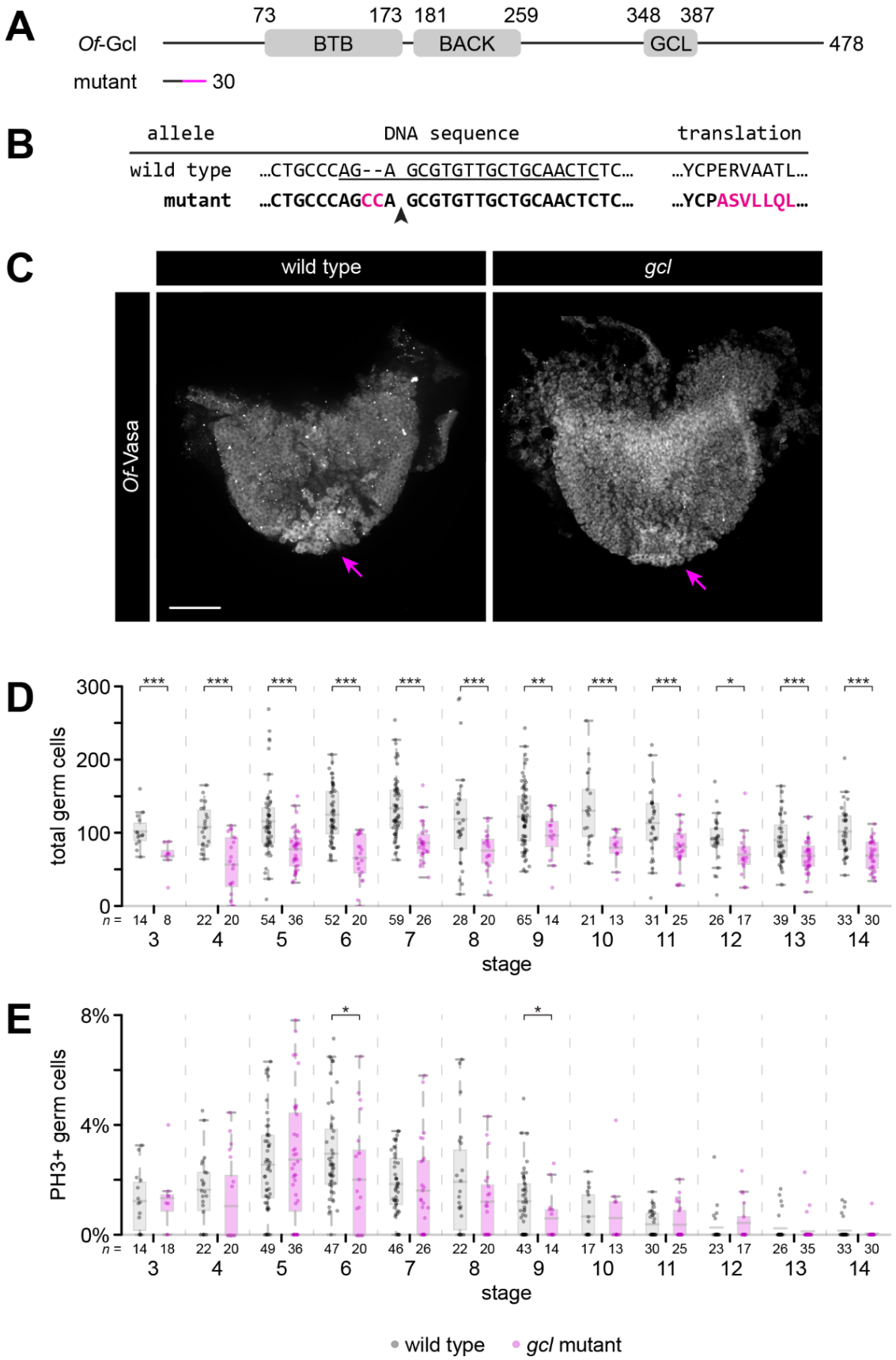
A
Of-Gcl
73
173
181
259
348
387
478
BTB
BACK
GCL
mutant
30
B
allele
DNA sequence
translation
wild type
…CTGCCCAG--A GCGTGTTGCTGCAACTCTC…
…YCPERVAATL…
mutant
…CTGCCCAGCCA GCGTGTTGCTGCAACTCTC…
…YCPASVLLQL…
C
wild type
gcl
Of-Vasa
D
total germ cells
300
200
100
0
n =
14 8
22 20
54 36
52 20
59 26
28 20
65 14
21 13
31 25
26 17
39 35
33 30
3
4
5
6
7
8
9
10
11
12
13
14
stage
E
PH3+ germ cells
8%
4%
0%
n =
14 18
22 20
49 36
47 20
46 26
22 20
43 14
17 13
30 25
23 17
26 35
33 30
3
4
5
6
7
8
9
10
11
12
13
14
stage
wild type
gcl mutant

Figure 2 (previous page). *Of-gcl* mutation decreases germ cell number in embryos.

(**A**) Predicted domain architecture of *Of*-Gcl and predicted mutant protein. Wild type *Of*-Gcl has two predicted folded domains (BTB and BACK domains) as well as a conserved motif called the GCL domain. The predicted mutant protein contains none of these domains and is truncated after residue 30.

(**B**) *Of-gcl* mutant allele contains a two base pair insertion, creating a frameshift and leading to a predicted truncated protein. Guide sequence is underlined; arrowhead marks predicted Cas9 cut site. Inserted bases and predicted mutated residues are indicated in magenta.

(**C**) Representative antibody stains against *Of*-Vasa to mark germ cells in stage 3 wild type and *gcl* mutant embryos. Mutant embryos still have germ cells at the expected location, indicated by arrows. Scale bar = 100 µm.

(**D**) Germ cell counts across embryogenesis in wild type and *gcl* mutant embryos. Mutant embryos have significantly fewer germ cells per embryo compared to wild type.

(**E**) Proportion of $PH3^+$ germ cells across embryogenesis in wild type and *gcl* mutant embryos. There is no significant difference in the proportion of proliferating germ cells between wild type and *gcl* mutant embryos.

All statistical tests are non-parametric bootstrap comparisons. Embryonic stages are defined in Supplemental Figure 1 and Supplemental Table 3. * $p < 0.05$; ** $p < 0.01$; *** $p < 0.001$

(1.5-column width)

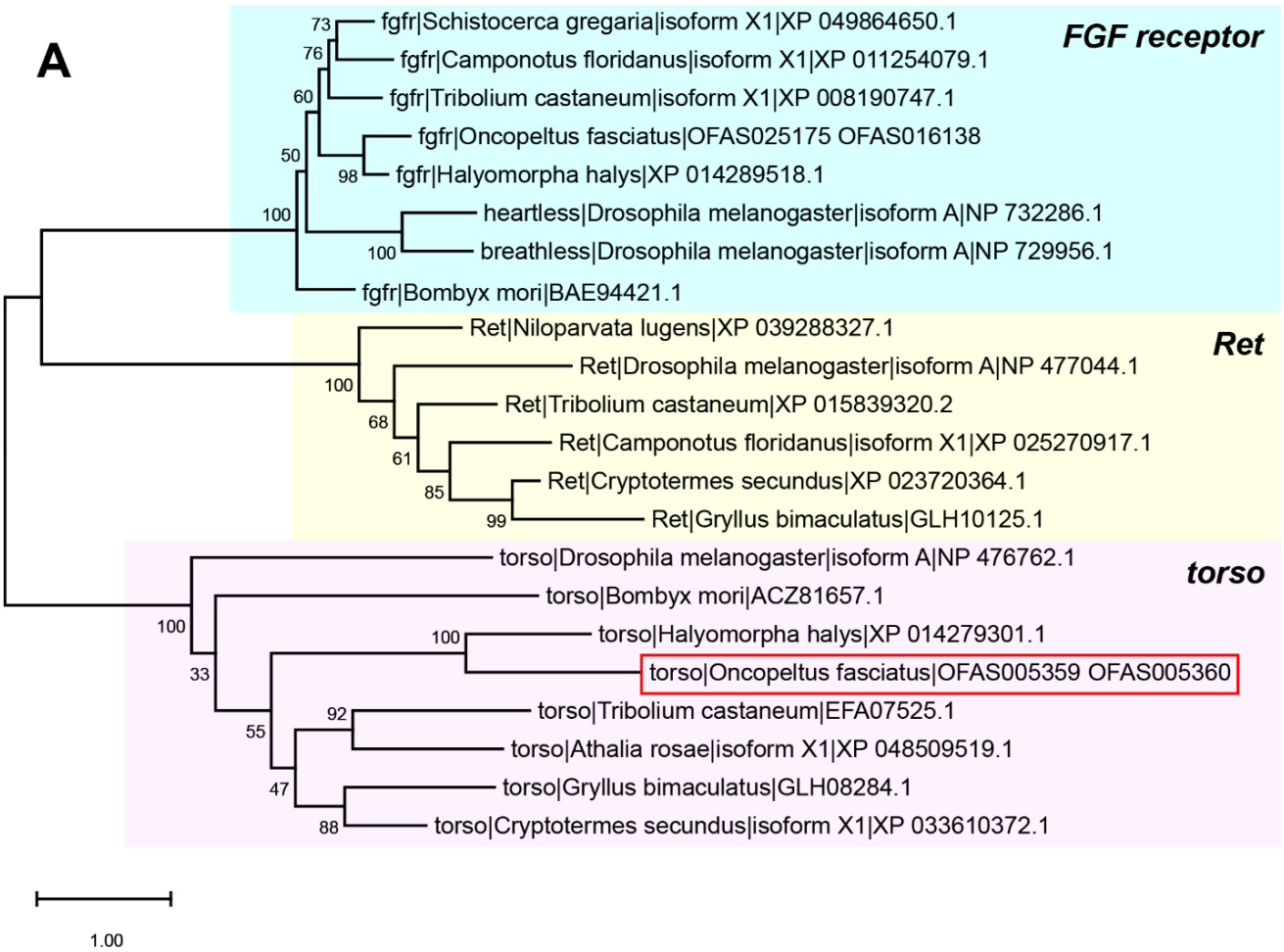
A
FGF receptor
fgfr|Schistocerca gregaria|isoform X1|XP 049864650.1
fgfr|Camponotus floridanus|isoform X1|XP 011254079.1
fgfr|Tribolium castaneum|isoform X1|XP 008190747.1
fgfr|Oncopeltus fasciatus|OFAS025175 OFAS016138
fgfr|Halyomorpha halys|XP 014289518.1
heartless|Drosophila melanogaster|isoform A|NP 732286.1
breathless|Drosophila melanogaster|isoform A|NP 729956.1
fgfr|Bombyx mori|BAE94421.1
Ret
Ret|Niloparvata lugens|XP 039288327.1
Ret|Drosophila melanogaster|isoform A|NP 477044.1
Ret|Tribolium castaneum|XP 015839320.2
Ret|Camponotus floridanus|isoform X1|XP 025270917.1
Ret|Cryptotermes secundus|XP 023720364.1
Ret|Gryllus bimaculatus|GLH10125.1
torso
torso|Drosophila melanogaster|isoform A|NP 476762.1
torso|Bombyx mori|ACZ81657.1
torso|Halyomorpha halys|XP 014279301.1
torso|Oncopeltus fasciatus|OFAS005359 OFAS005360
torso|Tribolium castaneum|EFA07525.1
torso|Athalia rosae|isoform X1|XP 048509519.1
torso|Gryllus bimaculatus|GLH08284.1
torso|Cryptotermes secundus|isoform X1|XP 033610372.1
1.00

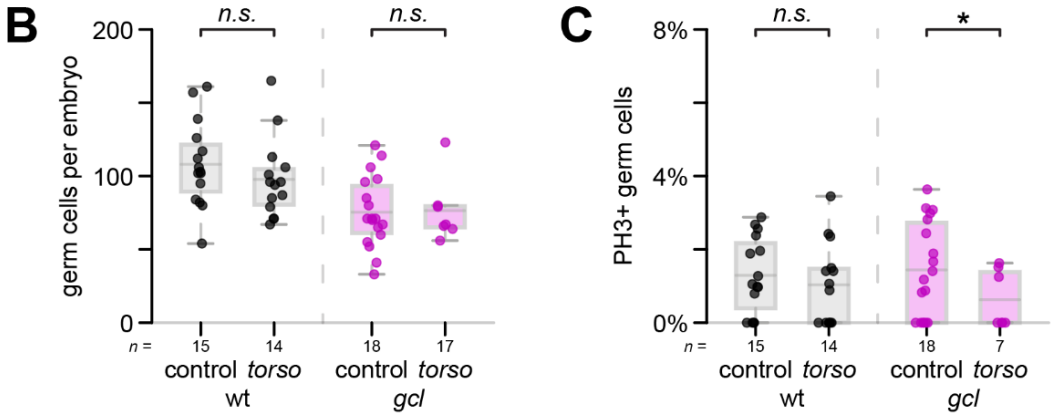
B
germ cells per embryo
n.s.
n.s.
n =
control torso
wt
control torso
gcl
C
PH3+ germ cells
n.s.
*

Figure 3 (previous page). *Of-torso* knockdown does not affect embryonic germ cell number.

(**A**) Phylogenetic analysis of *torso* and related receptor tyrosine kinases (*Ret oncogene* and *FGF receptor*) across insects. Each clade is individually highlighted for clarity. The putative *torso* homolog from *O. fasciatus* (OFAS005359/OFAS0005360) falls within the *torso* clade.

(**B**) Germ cell counts in stage 3–4 *Of-torso* RNAi embryos, performed in wild type and *gcl* mutant backgrounds. *torso* knockdown does not affect germ cell number in either background.

(**C**) Proportion of $PH3^+$ germ cells in stage 3–4 *Of-torso* RNAi embryos, performed in wild type and *gcl* mutant backgrounds. *torso* knockdown marginally reduces germ cell proliferation in *gcl* mutant embryos but not in wild type embryos.

All statistical tests are non-parametric bootstrap comparisons.
* $p < 0.05$; ** $p < 0.01$; *** $p < 0.001$

(full page width)

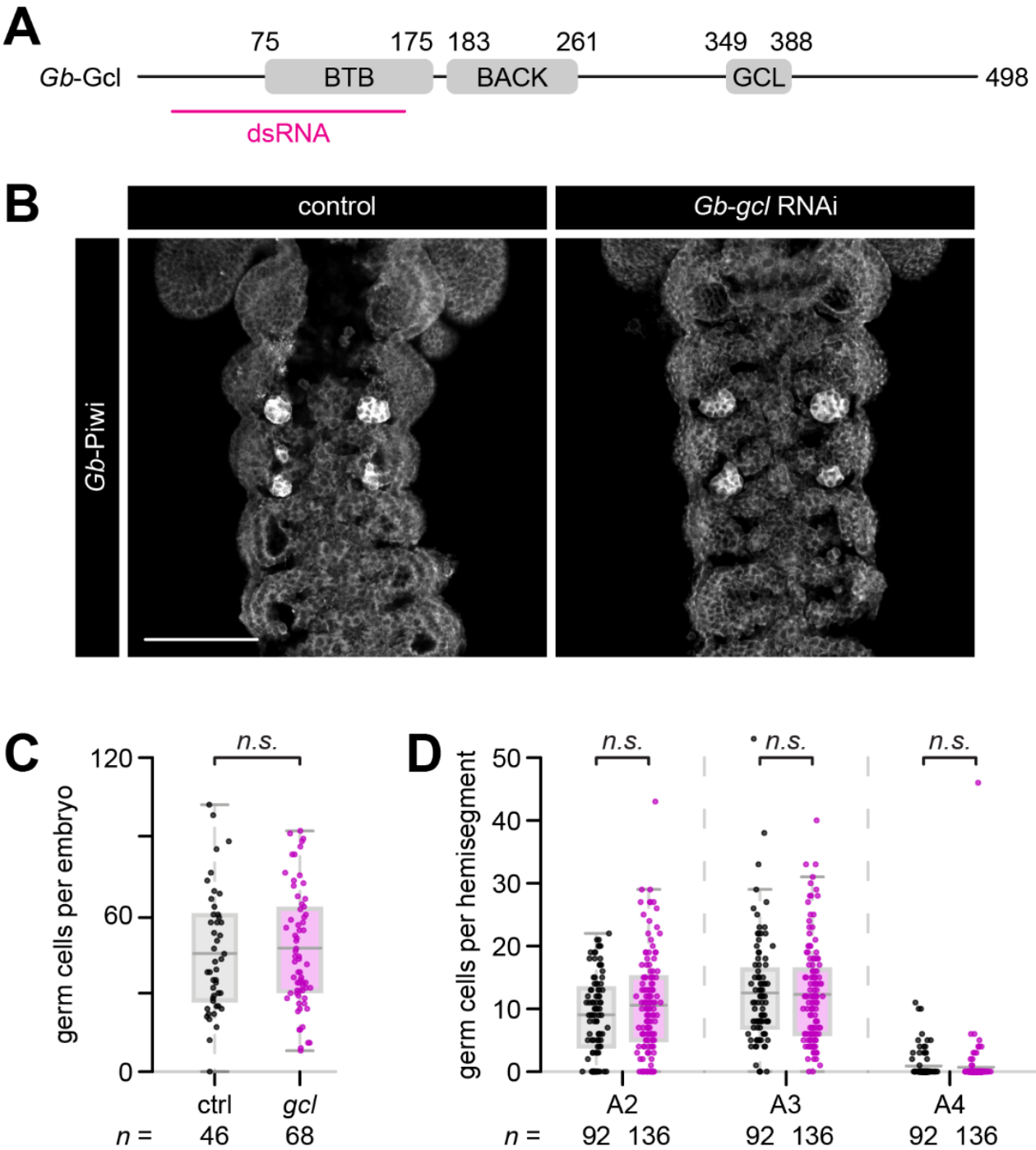
A
75
175
183
261
349
388
Gb-Gcl
BTB
BACK
GCL
498
dsRNA
B
control
Gb-gcl RNAi
Gb-Piwi
C
n.s.
germ cells per embryo
120
60
0
ctrl
gcl
n =
46
68
D
n.s.
n.s.
n.s.
germ cells per hemisegment
50
40
30
20
10
0
A2
A3
A4
n =
92
136
92
136
92
136

Figure 4 (previous page). *Gb-gcl* knockdown does not affect embryonic germ cell number.

(**A**) Predicted domain architecture of *Gb*-Gcl. *Gb*-Gcl has two predicted folded domains (BTB and BACK domains) and a conserved motif called the GCL domain. The fragment region used for dsRNA synthesis is marked.

(**B**) Representative antibody stains against *Gb*-Piwi to mark germ cells in stage 8 control and *gcl* knockdown embryos. Embryos in which *Gb-gcl* has been knocked down still have germ cells in the expected positions. Scale bar = 100 µm.

(**C**) Germ cell counts in stage 8 *Gb-gcl* RNAi embryos. Germ cell numbers are not significantly different in *Gb-gcl* knockdown embryos relative to controls. Each point represents one embryo.

(**D**) Germ cell counts in stage 8 *Gb-gcl* RNAi embryos, divided into hemisegments (*i.e.*, the left or right half of one segment). *Gb-gcl* knockdown does not affect the number of germ cells in any individual segment. Each point represents a hemisegment.

All statistical tests are non-parametric bootstrap comparisons.

(1.5 column width)

References

Abramson, J., Adler, J., Dunger, J., Evans, R., Green, T., Pritzel, A., Ronneberger, O., Willmore, L., Ballard, A.J., Bambrick, J., Bodenstein, S.W., Evans, D.A., Hung, C.-C., O'Neill, M., Reiman, D., Tunyasuvunakool, K., Wu, Z., Žemgulytė, A., Arvaniti, E., Beattie, C., Bertolli, O., Bridgland, A., Cherepanov, A., Congreve, M., Cowen-Rivers, A.I., Cowie, A., Figurnov, M., Fuchs, F.B., Gladman, H., Jain, R., Khan, Y.A., Low, C.M.R., Perlin, K., Potapenko, A., Savy, P., Singh, S., Stecula, A., Thillaisundaram, A., Tong, C., Yakneen, S., Zhong, E.D., Zielinski, M., Bapst, V., Kohli, P., Jaderberg, M., Hassabis, D., Jumper, J.M., 2024. Accurate structure prediction of biomolecular interactions with AlphaFold 3. Nature 630, 493–500. https://doi.org/10.1038/s41586-024-07487-w

Ansari, S., Troelenberg, N., Dao, V.A., Richter, T., Bucher, G., Klingler, M., 2018. Double abdomen in a short-germ insect: Zygotic control of axis formation revealed in the beetle,Tribolium castaneum. Proc. Natl. Acad. Sci. 115, 1819–1824. https://doi.org/10.1073/pnas.1716512115

Barnett, A.A., Nakamura, T., Extavour, C.G., 2019. Hox genes limit germ cell formation in the short germ insect,Gryllus bimaculatus. Proc. Natl. Acad. Sci. 116, 16430–16435. https://doi.org/10.1073/pnas.1816024116

Bregman, D.B., Du, L., Zee, S. van der, Warren, S.L., 1995. Transcription-dependent redistribution of the large subunit of RNA polymerase II to discrete nuclear domains. J. cell Biol. 129, 287–298. https://doi.org/10.1083/jcb.129.2.287

Butt, F.H., 1949. Embryology of the Milkweed Bug, Oncopeltus fasciatus (Hemiptera). Cornell Experiment Station Memoir 3–43.

Colonnetta, M.M., Lym, L.R., Wilkins, L., Kappes, G., Castro, E.A., Ryder, P.V., Schedl, P., Lerit, D.A., Deshpande, G., 2021. Antagonism between,germ cell-less,and Torso receptor regulates transcriptional quiescence underlying germline/soma distinction. eLife 10, e54346. https://doi.org/10.7554/elife.54346

Donoughe, S., Kim, C., Extavour, C.G., 2018. High-throughput live-imaging of embryos in microwell arrays using a modular specimen mounting system. Biol. Open 7, bio031260. https://doi.org/10.1242/bio.031260

Donoughe, S., Nakamura, T., Ewen-Campen, B., Green, D.A., Henderson, L., Extavour, C.G., 2014. BMP signaling is required for the generation of primordial germ cells in an insect. Proc. Natl. Acad. Sci. 111, 4133–4138. https://doi.org/10.1073/pnas.1400525111

Duncan, E.J., Benton, M.A., Dearden, P.K., 2013. Canonical terminal patterning is an evolutionary novelty. Dev. Biol. 377, 245–261. https://doi.org/10.1016/j.ydbio.2013.02.010

Edgar, R.C., 2004. MUSCLE: multiple sequence alignment with high accuracy and high throughput. Nucleic Acids Res. 32, 1792–1797. https://doi.org/10.1093/nar/gkh340

Ewen-Campen, B., Donoughe, S., Clarke, D.N., Extavour, C.G., 2013a. Germ cell specification requires zygotic mechanisms rather than germ plasm in a basally branching insect. Curr. Biol. 23, 835–842. https://doi.org/10.1016/j.cub.2013.03.063

Ewen-Campen, B., Jones, T.E.M., Extavour, C.G., 2013b. Evidence against a germ plasm in the milkweed bug,Oncopeltus fasciatus, a hemimetabolous insect. Biol. Open 2, 556–568. https://doi.org/10.1242/bio.20134390

Ewen-Campen, B., Schwager, E.E., Extavour, C.G., 2010. The molecular machinery of germ line specification. Mol. Reprod. Dev. 77, 3–18. https://doi.org/10.1002/mrd.21091

Extavour, C.G., Akam, M., 2003. Mechanisms of germ cell specification across the metazoans: epigenesis and preformation. Development 130, 5869–5884. https://doi.org/10.1242/dev.00804

Gupta, T., Extavour, C.G., 2013. Identification of a putative germ plasm in the amphipod,Parhyale hawaiensis. EvoDevo 4, 34. https://doi.org/10.1186/2041-9139-4-34

Huettner, A.F., 1923. The origin of the germ cells in,Drosophila melanogaster. J. Morphol. 37, 385–423. https://doi.org/10.1002/jmor.1050370204

Illmensee, K., Mahowald, A.P., 1974. Transplantation of posterior polar plasm in,Drosophila. Induction of germ cells at the anterior pole of the egg. Proc. Natl. Acad. Sci. 71, 1016–1020. https://doi.org/10.1073/pnas.71.4.1016

Jones, D.T., Taylor, W.R., Thornton, J.M., 1992. The rapid generation of mutation data matrices from protein sequences. Bioinformatics 8, 275–282. https://doi.org/10.1093/bioinformatics/8.3.275

Jongens, T.A., Ackerman, L.D., Swedlow, J.R., Jan, L.Y., Jan, Y.N., 1994. Germ cell-less encodes a cell type-specific nuclear pore-associated protein and functions early in the germ-cell specification pathway of Drosophila. Genes Dev. 8, 2123–2136. https://doi.org/10.1101/gad.8.18.2123

Jongens, T.A., Hay, B., Jan, L.Y., Jan, Y.N., 1992. The germ cell-less,gene product: A posteriorly localized component necessary for germ cell development in,Drosophila. Cell 70, 569–584. https://doi.org/10.1016/0092-8674(92)90427-e

Kimura, T., Ito, C., Watanabe, S., Takahashi, T., Ikawa, M., Yomogida, K., Fujita, Y., Ikeuchi, M., Asada, N., Matsumiya, K., Okuyama, A., Okabe, M., Toshimori, K., Nakano, T., 2003. Mouse Germ cell-less as an essential component for nuclear integrity. Mol. Cell. Biol. 23, 1304–1315. https://doi.org/10.1128/mcb.23.4.1304-1315.2003

Leatherman, J.L., Kaestner, K.H., Jongens, T.A., 2000. Identification of a mouse,germ cell-less,homologue with conserved activity in,Drosophila. Mech. Dev. 92, 145–153. https://doi.org/10.1016/s0925-4773(99)00335-4

Leatherman, J.L., Levin, L., Boero, J., Jongens, T.A., 2002. germ cell-less,acts to repress transcription during the establishment of the Drosophila germ cell lineage. Curr. Biol. 12, 1681–1685. https://doi.org/10.1016/s0960-9822(02)01182-x

Moore, J., Han, H., Lasko, P., 2009. Bruno negatively regulates,germ cell-less,expression in a BRE-independent manner. Mech. Dev. 126, 503–516. https://doi.org/10.1016/j.mod.2009.04.002

Nakamura, T., Extavour, C.G., 2016. The transcriptional repressor Blimp-1 acts downstream of BMP signaling to generate primordial germ cells in the cricket,Gryllus bimaculatus. Development 143, 255–263. https://doi.org/10.1242/dev.127563

Pae, J., Cinalli, R.M., Marzio, A., Pagano, M., Lehmann, R., 2017. GCL and CUL3 Control the Switch between Cell Lineages by Mediating Localized Degradation of an RTK. Dev. Cell 42, 130-142.e7. https://doi.org/10.1016/j.devcel.2017.06.022

Panfilio, K.A., Jentzsch, I.M.V., Benoit, J.B., Erezyilmaz, D., Suzuki, Y., Colella, S., Robertson, H.M., Poelchau, M.F., Waterhouse, R.M., Ioannidis, P., Weirauch, M.T., Hughes, D.S.T., Murali, S.C., Werren, J.H., Jacobs, C.G.C., Duncan, E.J., Armisén, D., Vreede, B.M.I., Baa-Puyoulet, P., Berger, C.S., Chang, C., Chao, H., Chen, M.-J.M., Chen, Y.-T., Childers, C.P., Chipman, A.D., Cridge, A.G., Crumière, A.J.J., Dearden, P.K., Didion, E.M., Dinh, H., Doddapaneni, H.V., Dolan, A., Dugan, S., Extavour, C.G., Febvay, G., Friedrich, M., Ginzburg, N., Han, Y., Heger, P., Holmes, C.J., Horn, T., Hsiao, Y., Jennings, E.C., Johnston, J.S., Jones, T.E., Jones, J.W., Khila, A., Koelzer, S., Kovacova, V., Leask, M., Lee, S.L., Lee, C.-Y., Lovegrove, M.R., Lu, H., Lu, Y., Moore, P.J., Munoz-Torres, M.C., Muzny, D.M., Palli, S.R., Parisot, N., Pick, L., Porter, M.L., Qu, J., Refki, P.N., Richter, R., Rivera-Pomar, R., Rosendale, A.J., Roth, S., Sachs, L., Santos, M.E., Seibert, J., Sghaier, E., Shukla, J.N., Stancliffe, R.J., Tidswell, O., Traverso, L., Zee, M. van der, Viala, S., Worley, K.C., Zdobnov, E.M., Gibbs, R.A., Richards, S., 2019. Molecular evolutionary trends and feeding ecology diversification in the Hemiptera, anchored by the milkweed bug genome. Genome Biol. 20, 64. https://doi.org/10.1186/s13059-019-1660-0

Robertson, S.E., Dockendorff, T.C., Leatherman, J.L., Faulkner, D.L., Jongens, T.A., 1999. germ cell-less,is required only during the establishment of the germ cell lineage of,Drosophila,and has activities which are dependent and independent of its localization to the nuclar envelope. Dev. Biol. 215, 288–297. https://doi.org/10.1006/dbio.1999.9453

Schoppmeier, M., Schröder, R., 2005. Maternal Torso Signaling Controls Body Axis Elongation in a Short Germ Insect. Curr. Biol. 15, 2131–2136. https://doi.org/10.1016/j.cub.2005.10.036

Skelly, J., Pushparajan, C., Duncan, E.J., Dearden, P.K., 2019. Evolution of the Torso activation cassette, a pathway required for terminal patterning and moulting. Insect Mol. Biol. 28, 392–408. https://doi.org/10.1111/imb.12560

Tamura, K., Stecher, G., Kumar, S., 2021. MEGA11: Molecular Evolutionary Genetics Analysis Version 11. Mol. Biol. Evol. 38, 3022–3027. https://doi.org/10.1093/molbev/msab120

Warren, S.L., Landolfi, A.S., Curtis, C., Morrow, J.S., 1992. Cytostellin: a novel, highly conserved protein that undergoes continuous redistribution during the cell cycle. J. Cell Sci. 103, 381–388. https://doi.org/10.1242/jcs.103.2.381

Weisbrod, A., Cohen, M., Chipman, A.D., 2013. Evolution of the insect terminal patterning system—Insights from the milkweed bug,Oncopeltus fasciatus. Dev. Biol. 380, 125–131. https://doi.org/10.1016/j.ydbio.2013.04.030

Ylla, G., Nakamura, T., Itoh, T., Kajitani, R., Toyoda, A., Tomonari, S., Bando, T., Ishimaru, Y., Watanabe, T., Fuketa, M., Matsuoka, Y., Barnett, A.A., Noji, S., Mito, T., Extavour, C.G., 2021. Insights into the genomic evolution of insects from cricket genomes. Commun. Biol. 4, 733. https://doi.org/10.1038/s42003-021-02197-9